Journal of Aerosol Science 151 (2021) 105670

Contents lists available at ScienceDirect

Journal of Aerosol Science

journal homepage: http://www.elsevier.com/locate/jaerosci

Approximated expression of the hygroscopic growth factor for polydispersed aerosols

Chang H. Jung [a,*], Young Jun Yoon [b], Junshik Um [c], Seoung Soo Lee [d], Kyung Man Han [e], Hye Jung Shin [f], Ji Yi Lee [g], Yong Pyo Kim [h]

[a] Department of Health Management, Kyungin Women's University, Incheon, 21041, Republic of Korea
[b] Korea Polar Research Institute, Incheon, 21990, Republic of Korea
[c] Department of Atmospheric Sciences, Pusan National University, Busan, 46241, Republic of Korea
[d] Earth System Science Interdisciplinary Center, University of Maryland, College Park, MD, 20740, USA
[e] School of Earth Sciences and Environmental Engineering, Gwangju Institute of Science and Technology, Gwangju, 61005, Republic of Korea
[f] Climate and Air Quality Research Department, National Institute of Environmental Research, Incheon, 22689, Republic of Korea
[g] Department of Environmental Science and Engineering, Ewha Womans University, Seoul, 03760, Republic of Korea
[h] Department of Chemical Engineering and Materials Science, Ewha Womans University, Seoul, 03760, Republic of Korea

ARTICLE INFO

Keywords:
Analytical approximated expression
Polydispersed aerosol
Hygroscopic growth factor
Aerosol size distribution
Scattering enhancement factor

ABSTRACT

Hygroscopic growth of aerosols plays an important role in the characterization of atmospheric aerosols. Physico-chemical and optical properties of aerosols are dependent on relative humidity (RH) as well as on their size and composition. In this study, scattering enhancement factors, f (RH), for polydispersed aerosols were approximated. f(RH) of ammonium sulfate and ammonium nitrate (AS) and NaCl aerosols (ss) were considered under the assumption of externally mixed aerosols. f(RH) was calculated using the Mie theory for polydispersed aerosols at a given RH and corresponding water uptake (denoted as $f_{Mie}(RH)$). f(RH) was approximated as a quadratic function of RH (denoted as $f_{app}(RH)$). The obtained approximated f(RH) or $f_{app}(RH)$) values were compared with the values based on the Mie theory and showed a reasonable agreement between them. To the best of our knowledge, this is the first study that parametrizes the size dependency of f(RH) for log normally distributed aerosols.

1. Introduction

Light absorption and scattering are the main processes involved in the interaction between aerosol particles and solar radiation (Ghan et al., 2012; Leibensperger et al., 2012). One of the essential aerosol characteristics in terms of interaction is hygroscopicity. The hygroscopic growth of aerosols is important in the interpretation of aerosol variables, such as visibility and aerosol optical depth (AOD) (Cheng et al., 2008; Liu et al., 2020). Hygroscopicity characterizes the ability of aerosols to take up water under subsaturated and supersaturated conditions and is a key parameter in determining the direct and indirect effects of aerosols on climate (Ogawa et al., 2016; Swietlicki et al., 2008; IPCC, 2013; Zhang et al., 2014). At an elevated ambient relative humidity (RH), hygroscopic aerosols have larger scattering cross sections than non-hygroscopic aerosols (Twohy et al., 2009). The hygroscopic growth of aerosols is specified by the growth factor (GF). The GF is defined to be the ratio of the wet particle radius to the dry particle radius, and can be

* Corresponding author.
E-mail address: jch@kiwu.ac.kr (C.H. Jung).

https://doi.org/10.1016/j.jaerosci.2020.105670
Received 26 March 2020; Received in revised form 5 September 2020; Accepted 8 September 2020
Available online 16 September 2020

calculated as a function of RH (Eichler et al., 2008; Kreidenweis et al., 2008; Sorooshian et al., 2008):

$$GF(RH) = \frac{d_{wet}(RH)}{d_{dry}} = \left(\frac{V_{wet}(RH)}{V_{dry}}\right)^{1/3} = \left(\frac{V_{dry} + V_{water}(RH)}{V_{dry}}\right)^{1/3} = \left(1 + \frac{V_{water}(RH)}{V_{dry}}\right)^{1/3} \quad (1)$$

where, d_{wet}, d_{dry}, V_{wet}, V_{dry}, and V_{water} are the diameters and volumes of wet and dry aerosols and water, respectively.

To quantify the effect of hygroscopic growth on aerosol scattering, the scattering enhancement factor as a function of RH, which is f (RH), is defined as follows (Lagrosas et al., 2019; Pitchford et al., 2007; Zhang et al., 2014; Zieger et al., 2010):

$$f(RH) = \frac{b_{ext}(RH)}{b_{ext}(dry)} \quad (2)$$

where b_{ext}(RH) and b_{ext}(dry) are the aerosol light extinction coefficients under enhanced RH conditions and dry conditions, respectively, and

$$b_{ext} = \int Q_{ext}(d_p)\frac{\pi}{4}d_p^2 n(d_p)dd_p \quad (3)$$

In Eq. (3), Q_{ext} is the single particle extinction efficiency and d_p is the particle diameter. Quantification of f(RH) is critical to determine the response of aerosol optical properties to hygroscopic growth at various ambient RH and model the direct aerosol effect. Many previous studies have investigated aerosol hygroscopicity and associated growth through measurements and theoretical modeling (Liu et al., 2013; Zieger et al., 2010; 2011; 2013; 2014). These studies have mainly focused on the relationships among optical properties (such as aerosol scattering coefficients, radiative forcing, visibility), chemical species, and RH (Eichler et al., 2008; Kuang et al., 2016; Liu et al., 2008, 2013; Malm & Day, 2001; Malm et al., 2005; Cheng et al., 2008, 2003; Pan et al., 2009). There have also been many studies on the parameterization of these relations and the associated aerosol hygroscopicity, describing the variation in f(RH) with RH (Carrico et al., 2003; Chen et al., 2014; Deng et al., 2016; Hänel, 1981; Im et al., 2001; Sheridan et al., 2002; Kasten, 1969; Kiehl et al., 2000; Kotchenruther & Hobbs, 1998; Kreidenweis et al., 2005; Malm et al., 1994; Petters & Kreidenweis, 2007; Randriamiarisoa et al., 2006; Rissler et al., 2006; Titos et al., 2016; Xu et al., 2002; Yan et al., 2009; Zhang et al., 2015; Zieger et al., 2011). Titos et al. (2016) reviewed several empirical parameterizations for the relationship between f(RH) and RH and tested them using experimental data for hygroscopic growth. They also discussed the potential error sources in f(RH) and found the error to be around 20–40% for moderately hygroscopic aerosols. Most of these previous parameterizations are based on empirically fitted functions.

Generally, observational f(RH) can be obtained by measuring dry and wet scattering efficiencies using an optical instrument, such as a nephelometer (Cheng et al., 2008; Zhang et al., 2008). A theoretical f(RH) can be estimated from dry and wet scattering efficiencies based on the Mie theory (Tao et al., 2017; Liu et al., 2008; Zieger et al., 2010; 2011). The Interagency Monitoring of Protected Visual Environments (IMPROVE) network measures scattering coefficients using nephelometry (Malm et al., 1994). One of the widely used expressions for the extinction coefficient, as a function of the aerosol mass concentration and f(RH), is the reconstructed equation proposed by Malm et al. (1994), of which there are many different versions (Hand et al., 2019; Hand & Malm, 2007; Malm & Day, 2001; Malm et al., 1994; Malm et al., 2000). According to Malm et al. (1994), a scattering and absorption coefficient can be expressed as:

$$b_{scat} = 3.0\left\{C_{(NH_4)_2SO_4} + C_{NH_4NO_3}\right\}f_{AS}(RH) + 4.0C_{OMC} + C_{soil} + 0.6C_{CM} + 1.37f_{ss}(RH)C_{ss},\ b_{abs} = 10.0C_{BC} \quad (4)$$

where, b_{scat} and b_{abs} (in Mm^{-1}) are the reconstructed scattering and absorption coefficients, and $C_{(NH_4)_2SO_4}$, $C_{NH_4NO_3}$, C_{OMC}, C_{soil}, C_{CM}, C_{ss}, C_{BC}denote the mass concentrations of ammonium sulfate, ammonium nitrate, organic aerosol, soil, coarse mode particles, NaCl, and black carbon (BC) respectively. Here, the unit of mass concentration is $\mu g/m^3$, f_{AS} (RH) denotes the scattering enhancement factor of AS (ammonium sulfate and ammonium nitrate), and f_{SS}(RH) denotes that of NaCl. It should be noted that sulfate and nitrate aerosols have the same f_{AS}(RH) in Malm's equation (Malm et al., 1994). Malm's reconstructed equation assumes a single f_{AS}(RH) or f_{SS}(RH), which is independent of particle size.

As discussed, one of the main drawbacks of Malm's equations is that they are unable to consider the size-dependent f(RH), which is an important aspect of aerosol hygroscopicity (Pitchford et al., 2007; Chen et al., 2014; Laskina et al., 2015; Wang et al., 2018). For a given RH and chemical composition, different aerosol size distributions should yield different growth rates. Thus, f_{AS}(RH) and f_{SS}(RH), which comprise f(RH) in Eq. (4) should be expressed as a function of particle size as well as particle composition and refractive index. Most previous studies, however, did not consider size-dependent effects due to the complexity in reflecting polydispersity and assumed f(RH) to be constant at varying aerosol diameters (Molnár et al., 2020; Pitchford et al., 2007). However, many theoretical and empirical studies prove a size dependency and suggest that individual chemical substances should be specifically assessed with respect to particle size (Eichler et al., 2008; Liu et al., 2013; Chen et al., 2014; Wang et al., 2018; Qi et al., 2018; Shen et al., 2018; Zhang et al., 2018). From a theoretical point of view, when a size-dependent f(RH) is to be considered, f(RH) should be recalculated for each RH using a thermodynamic model and the Mie theory for each size distribution. Yet, such a recalculation is very complicated and, thus, instead of adopting this theoretical approach, simple parameterizations of hygroscopic growth factors for polydisperse aerosols need to be developed.

To consider size-dependent effects, Pitchford et al. (2007) revised the IMPROVE equation for fine- and accumulation-mode particles using the Mie theory. They used a bimodal aerosol size distribution with geometric mean diameters of 0.2 and 0.5 μm (geometric

standard deviation [GSDs] of 2.2 and 1.5, respectively) for fine and accumulation modes, respectively. Although their study used different f(RH) for fine and accumulation modes (Pitchford et al., 2007), it did not consider the varying polydispersed size and changes in the size distribution.

In this study, an analytical approach to the approximated formula for the f(RH) of the polydisperse size distribution of AS and NaCl was developed. For this development, we assumed that aerosols follow the lognormal size distribution (Jung et al., 2018, 2019; Seinfeld & Pandis, 1998).

In the following, the calculation of f(RH) using the Mie theory (denoted as $f_{Mie}(RH)$) and the procedure of parameterizing f(RH) using approximation (denoted as $f_{app}(RH)$) are described. Moreover, the parameterized and calculated f(RH) values are compared and discussed. This new trial to parametrize the size dependency of f(RH) enables the investigation of aerosol hygroscopic properties, such as AOD, visibility, and other related optical properties.

2. Materials and methods

2.1. Calculating f(RH) using the Mie model ($f_{Mie}(RH)$)

Two step approach was used to obtain analytic approximations of the scattering enhancement factor: 1) calculating f(RH) using the Mie theory ($f_{Mie}(RH)$), and 2) estimating f(RH) using approximation ($f_{app}(RH)$) through multilinear regressions (MLR). Fig. 1 shows the procedures of those two steps. Spherical particles with an external mixture were assumed for the calculation under the particle size distribution and the complex particle refractive index at a wavelength of 0.55 μm (Malm et al., 1994). Here, the refractive index of AS and NaCl is 1.53 and 1.55, respectively (Malm, 2016; Pitchford et al., 2007).

b_{ext}(dry) was calculated using the Mie theory with the dry size distribution and refractive index. $b_{ext}(RH)$ was calculated by applying GF(RH) to the size distribution using the Mie theory, which accounts for the change in particle volume and refractive index from the addition of water.

A dry log-normal size distribution with GSDs of 1.5, 2.0, and 2.5 was considered in order to consider broad ranges of aerosol size distribution (Ghan & Zaveri, 2007; Jung et al., 2019; Musante et al., 2002). The GF(RH) and water contents were calculated based on the Aerosol Inorganics Model (AIM), which is a thermodynamic equilibrium model with the "no solids" option of pure AS and NaCl (Clegg et al., 2003). A more detailed description of the Mie-based calculation of f(RH) can be found in related studies (Zieger et al., 2010; 2014; van de Hulst, 1981; Lin et al., 2014). Hysteresis is the deliquescence branch with an abrupt increase in the water volume at the deliquescence RH (DRH), and the efflorescence branch with an abrupt evaporation at the crystallization relative humidity (CRH) (Pitchford et al., 2007; Randriamiarisoa et al., 2006). According to Pitchford et al. (2007), deliquescence is rarely observed in the

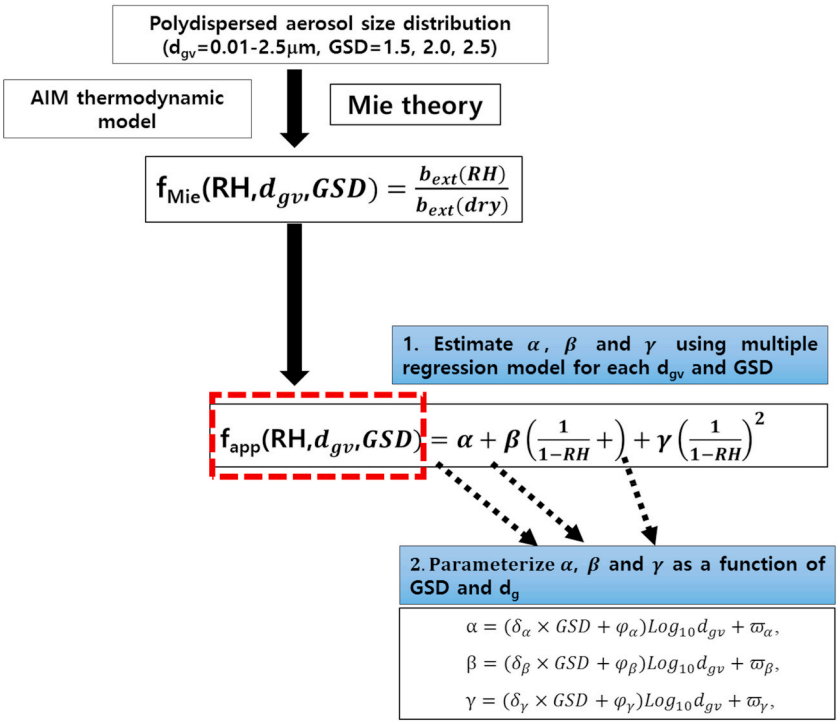

Fig. 1. Schematic of processes for obtaining the analytic expressions of the aerosol mass concentration and scattering enhancement factor, f(RH), of polydispersed aerosols. GSD represents the geometric standard deviation, RH is the relative humidity, and AIM stands for aerosol thermodynamic model.

environment. We used the efflorescence growth curve for AS and NaCl. Because pure AS crystallizes at 37% RH, it is assumed that there is no hygroscopic growth, and that the f(RH) is 1.0 below this RH. The water absorption curves for sea salt were nearly identical to those for NaCl. Below the crystallization point (i.e., RH 47% for NaCl), the growth factor was set to 1.0. Based on the growth curve, f (RH) was introduced to illustrate the variability of the bulk scattering properties of aerosols at ambient RH, relative to a dry condition (Covert et al., 1972; Zieger et al., 2010).

2.2. Parameterization of f(RH) using approximation ($f_{app}(RH)$)

Table 1 shows a comparison of the different types of parameterized expressions for f(RH) (Kasten, 1969; Kotchenruther & Hobbs, 1998; Malm et al., 1994; Day et al., 2000; Kiehl et al., 2000; Im et al., 2001; Sheridan et al., 2001; Xu et al., 2002; Carrico et al., 2003; Liu et al., 2008, 2009; Yan et al., 2009; Pan et al., 2009; Zieger et al., 2011; Zhang et al., 2015; Chen et al., 2014; Deng et al., 2016).

IMPROVE uses approach by Malm et al. (1994). In this study, we approximated $f_{Mie}(RH)$ as a quadratic function of $\left(\frac{1}{1-RH}\right)$ for AS and NaCl (Malm et al., 1994; Deng et al., 2016).

$$f_{app,AS}(RH) = \alpha_{AS} + \beta_{AS}\left(\frac{1}{1-RH}\right) + \gamma_{AS}\left(\frac{1}{1-RH}\right)^2 \tag{5a}$$

$$f_{app,ss}(RH) = \alpha_{ss} + \beta_{ss}\left(\frac{1}{1-RH}\right) + \gamma_{ss}\left(\frac{1}{1-RH}\right)^2 \tag{5b}$$

$f_{Mie}(RH)$ was calculated using the Mie theory, with different aerosol size distributions. We approximated $f_{Mie}(RH)$ as linear combinations of $\left(\frac{1}{1-RH}\right)$ and $\left(\frac{1}{1-RH}\right)^2$ using multilinear regression (MLR). MLR is a statistical technique that uses several independent (explanatory) variables to predict the outcome of a dependent variable.

Here, the dependent variable is $f_{Mie}(RH)$ and the independent variables are $\left(\frac{1}{1-RH}\right)$ and $\left(\frac{1}{1-RH}\right)^2$.

α is the intercept, β, and γ are slope coefficients for the explanatory variable, and the subscripts AS and ss denote AS and NaCl. Using α β, and γ, we can obtain the approximated f(RH) ($f_{app}(RH)$) from Eq. (5). The coefficients were obtained by applying MLR to the $f_{Mie}(RH)$ values computed for the range of aerosol size distributions. These coefficients were statistically significant at a 0.05 significance level ($p < 0.05$).

The estimated coefficients (α β, and γ) vary with the aerosol size distribution. For a given GSD, α β, and γ can be approximated by functions of the volume-mean diameter.

$$\gamma = \eta_\gamma Log_{10}\left(d_{gv} / d_{g0}\right) + \varpi_\gamma \tag{6}$$

Table 1
Parameterized expressions for the aerosol scattering enhancement factor, $f_{app}(RH)$.

f(RH)	empirical coefficients	References
$f_{app}(\mathrm{RH}) = \exp\left[c_1 + \left(\frac{c_2}{RH+c_3}\right) + \left(\frac{c_4}{RH+c_5}\right)\right]$	c_1, c_2, c_3, c_4, c_5	Kiehl et al. (2000); Im et al. (2001)
$f_{app}(\mathrm{RH}) = 1 + a \times RH^b$	a, b	Kotchenruther and Hobbs (1998); Carrico et al. (2003); Zhang et al. (2015)
$f_{app}(\mathrm{RH}) = \left(\frac{1}{1-RH}\right)^\gamma$	γ	Kotchenruther and Hobbs (1998)
$f_{app}(\mathrm{RH}) = a\left(\frac{1}{1-RH}\right)^\gamma$	γ	Kasten (1969); Carrico et al. (2003); Zieger et al. (2011); Xu et al. (2002); Yan et al. (2009); Liu et al. (2008, 2009); Pan et al. (2009)
$f_{app}(\mathrm{RH}) = \left(\frac{1-RH}{1-RH_{ref}}\right)^\gamma$	γ	Sheridan et al. (2001)
$f_{app}(\mathrm{RH}) = a\left(\frac{1}{1-RH}\right)^{b\times RH}$	a, b	Chen et al. (2014)
$f_{app}(\mathrm{RH}) = (1 + 2.42 \times RH^{4.67}) + 0.062 \times (1-RH)^{-0.82}$		Liu et al. (2009)
$f_{app}(\mathrm{RH}) = \left(1 + \kappa\frac{RH}{1-RH}\right)$	κ	Brock et al. (2016)
$f_{app}(\mathrm{RH}) = \alpha + \beta\left(\frac{1}{1-RH}\right) + \gamma\left(\frac{1}{1-RH}\right)^2$	α, β, γ	Malm et al. (1994); Deng et al. (2016); Present study
$f_{app}(\mathrm{RH}) = \alpha + \beta RH + \gamma RH^2$	α, β, γ	Kreidenweis et al. (2005); Ghan and Zaveri (2007)
$f_{app}(\mathrm{RH}) = \frac{a + bRH}{1 + cRH}$	a, b, c	Day et al. (2000)

where, η_α η_β η_γ ϖ_α ϖ_β, and ϖ_γ are coefficients for α β, and γ, dgv is the volume-mean diameter in μm, and dgo is the unit diameter (=1 μm). Here, all the logarithms of dimensioned quantities were standardized to avoid confusion with units (Matta et al., 2011).

Fig. 2 shows the coefficients for $f_{AS}(RH)$ as a function of the log10dgv. GSDs of 1.5, 2.0, and 2.5 were considered. For a small aerosol-size range (dgv < 0.03 μm), the coefficients α, β, and γ converge to 0.3, 0.83, and 0.07, respectively. Meanwhile, for large particles that are >1 μm in volume-mean diameter (dgv > 1 μm), the coefficients α, β, and γ converge to 0.85, 0.28, and 0.0, respectively. In these cases, η_α, η_β, and η_γ should be 0 in Eq. (6). An intermediate size exists between the two size ranges (0.03 μm < dgv < 1 μm); the approximations for this intermediate size vary with size, meaning that they should be expressed as dgv and GSD, as shown in Fig. 2. Coefficients for the intermediate size can be approximated by the linear function log10(dgv/dg0), as described in Eq. (6). For example, the intercept coefficient αAS (α for AS) can be approximated to be 0.49Log10(dgv/dg0)+0.84, 0.35Log10(dgv/dg0)+0.84, and 0.22Log10(dgv/dg0)+0.84 for a GSD of 1.5, 2.0, and 2.5, respectively.

Fig. 3 shows the coefficients for $f_{ss}(RH)$. The calculated and approximated results for αss, βss, and γss were compared for the GSDs of 1.5, 2.0, and 2.5, respectively. αss, βss, and γss can be approximated by the linear function log10(dgv/dg0) (Fig. 3). For example, αss can be approximated to be 1.3Log10(dgv/dg0)+1.4 and 0.88Log10(dgv/dg0)+1.4 for GSDs of 1.5 and 2.0 in the intermediate sizes (0.03 μm < dgv< 1 μm), respectively, and converges to 0.0 and 1.35 for small (dgv < 0.03 μm) and large particles (dgv > 1 μm), respectively.

To consider polydispersity with different GSDs, we required more parameterizations for the coefficients η_α η_β, and η_γ in Eq. (6) in the intermediate-size range. Here η_α η_β, and η_γ can be estimated by linear fitting as a function of the GSD with the slope (δ) and intercept (ϕ). Finally, we approximated η_α, η_β, and η_γ again as a function of GSD, as shown in Eq. (7).

$$\eta_\alpha = \delta_\alpha \times GSD + \phi_\alpha$$

$$\eta_\beta = \delta_\beta \times GSD + \phi_\beta$$

$$\eta_\gamma = \delta_\gamma \times GSD + \phi_\gamma \tag{7}$$

Fig. 4 shows the approximated estimation of the slope coefficients (η_α η_β, and η_γ) as a function of GSD for AS and NaCl. η_α, η_β, and η_γ for the intermediate sizes can be approximated as (−0.27GSD+0.89), (0.29GSD-0.94), and (0.03GSD-0.085) for AS, and (−0.68GSD+2.29), (0.7GSD −2.77), and (0.31GSD-0.91) for NaCl, respectively.

Then, the resultant coefficients for the polydispersed aerosol with f_{app}(RH) were expressed as a function of the d_{gv} and GSDby

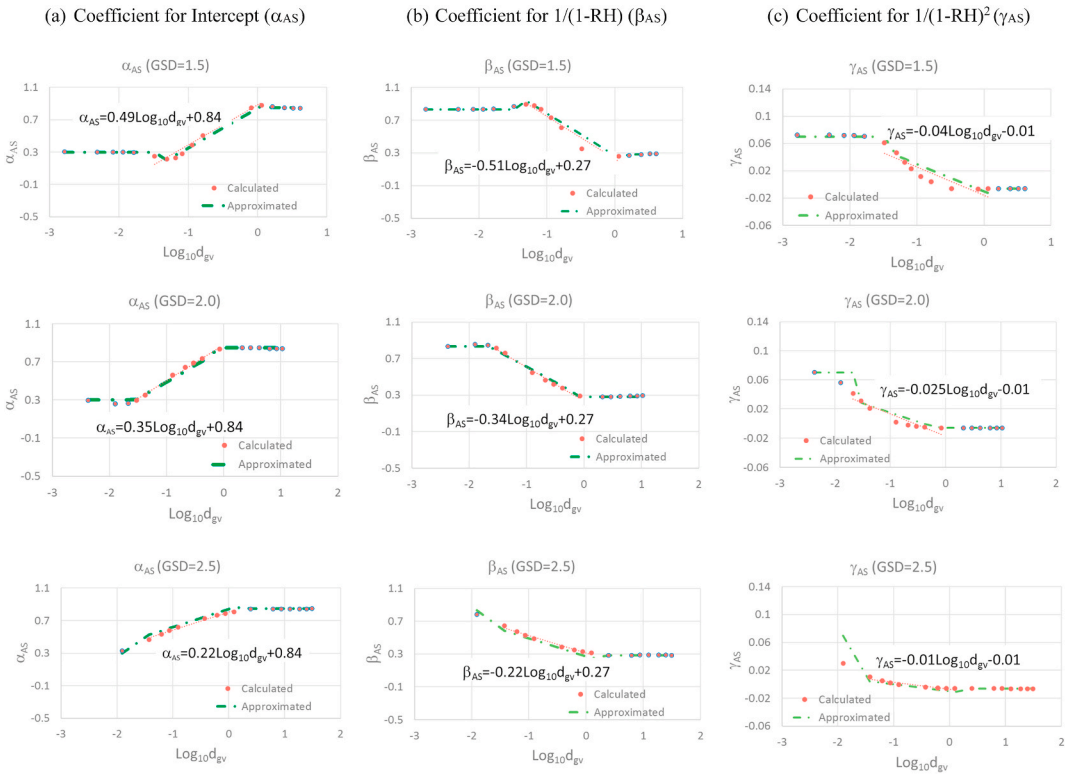

Fig. 2. Coefficients of the aerosol mass concentration and scattering enhancement factor, f(RH), of AS (ammonium sulfate and ammonium nitrate aerosols) as a function of the volume-mean diameter (d_{gv}) and geometric standard deviation (GSD). Circles are calculated coefficients and dotted and dash-dot lines are approximated coefficients.

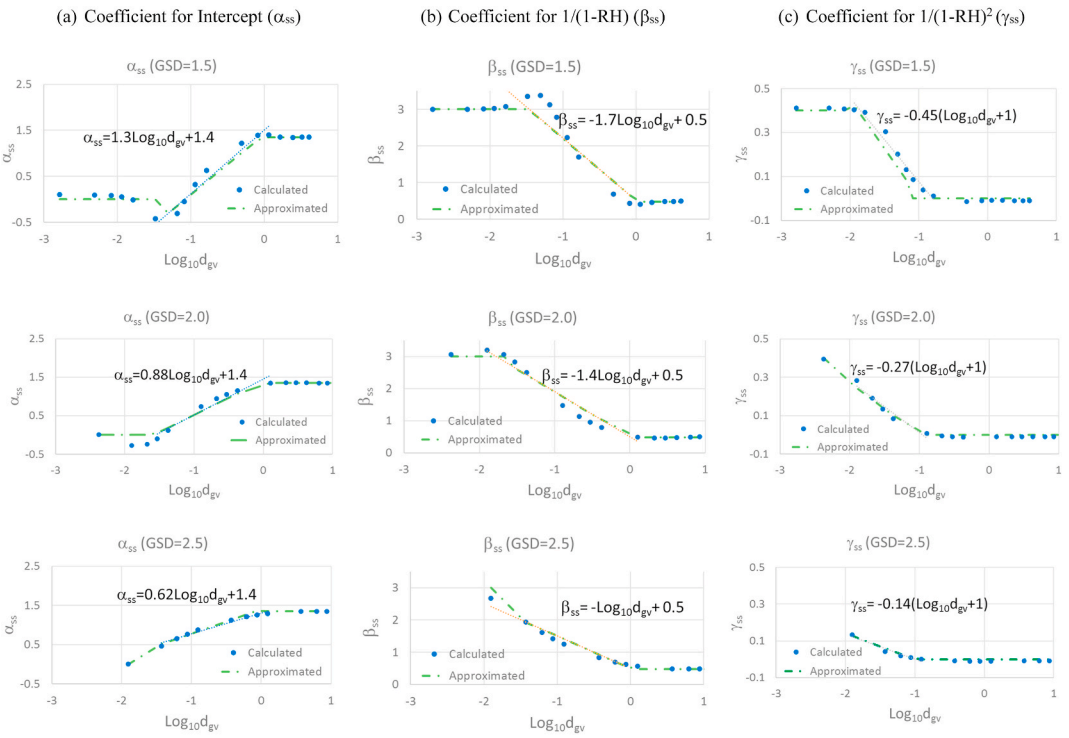

Fig. 3. Coefficients of the aerosol mass concentration and scattering enhancement factor, f(RH), of NaCl as a function of the volume-mean diameter (d_{gv}) and geometric standard deviation (GSD). Circles are calculated coefficients and dotted and dash-dot lines are approximated coefficients.

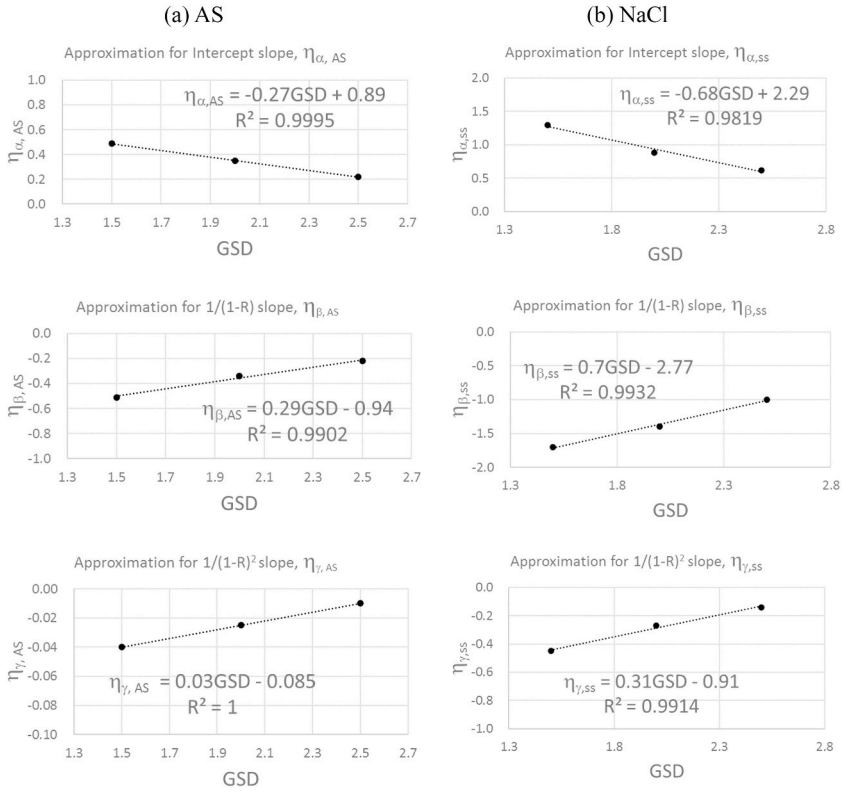

Fig. 4. Approximated estimation for the slope of each of the coefficients (α, β, γ) as a function of GSD for AS and NaCl.

combining Eqs. (6) and (7) as follows:

$$\alpha = (\delta_\alpha \times GSD + \phi_\alpha) Log_{10}\left(d_{gv} / d_{g0}\right) + \varpi_\alpha$$

$$\beta = (\delta_\beta \times GSD + \phi_\beta) Log_{10}\left(d_{gv} / d_{g0}\right) + \varpi_\beta$$

$$\gamma = (\delta_\gamma \times GSD + \phi_\gamma) Log_{10}\left(d_{gv} / d_{g0}\right) + \varpi_\gamma \quad (8)$$

The approximated subsequent expressions and detailed coefficients for each d_{gv}, d_g, and GSD are summarized in Tables 2 and 3 for AS and NaCl, respectively. It has to be noted that the parameterization in this study is based on d_{gv}. However, d_{gv} can be converted to the number-mean diameter (d_g). The relationship between d_g and d_{gv} can be expressed as follows (Hinds, 1999).

$$d_{gv} = d_g \exp\left[3ln^2(GSD)\right] \quad (9)$$

While d_{gv} is useful for volume-size distributions that are, in turn, useful when dealing with air quality and optical properties of aerosols, d_g is useful for number-size distributions that are, in turn, useful when dealing with microphysical processes.

3. Results and discussion

3.1. Comparison of approximated results with those from the Mie theory

Fig. 5 shows f(RH) for different size distributions with different GSDs and d_g for AS, with an RH of 37–95%. Fig. 5(a) shows the f_{Mie}(RH) with a GSD of 1.5 and different d_g of 0.05, 0.1, 0.2, and 0.7 μm. As shown in Fig. 5(a), f_{Mie}(RH) decreases as d_g increases. Fig. 5 (a) also shows that the original f(RH) from Malm et al. (1994), which was parameterized based on the data published by Tang et al. (1981), is between the f(RH) values varying with d_g for a given RH and GSD.

Fig. 5(b) shows the f_{Mie}(RH) with the different GSDs of 1.5 and 2.5. f_{Mie}(RH) converges as the GSD increases, regardless of particle size. For a GSD of 2.5, the f(RH) with a d_g of 0.1 μm is similar to that with a d_g of 0.7 μm. Fig. 5(c) and (d) show a comparison between the Mie-calculated (f_{Mie}(RH)) and approximated f(RH) (f_{app}(RH)). Fig. 5(c) and (d) show the comparison between the d_g of 0.1 and 0.7 μm for GSDs of 1.5 and 2.5, respectively. The Mie calculated and approximated results show a good agreement. The mean absolute errors (MAE) were 13.07% for a d_g of 0.1 μm with a GSD of 1.5, 9.97% for a dg of 0.7 μm with a GSD of 1.5, 12.6% for a dg of 0.1 μm with a GSD of 2.5, and 6.17% for a dg of 0.7 μm with a GSD of 1.5 over the RH range of 37–95%. MAE represents the average of the absolute differences between prediction and actual observation across the test samples, where all individual differences are equally weighted. It measures the average magnitude of errors in a set of predictions, without considering their direction (Habyarimana et al., 2019). Here, MAE is the average of the absolute difference over the RH range between the approximated and Mie calculated results.

$$MAE(a-b) = \frac{1}{n}\sum_{RH=a}^{b}\frac{\left|X_{Mie,RH} - X_{app,RH}\right|}{X_{Mie,RH}} \quad (10)$$

where, $X_{Mie,RH}$ and $X_{app,RH}$ are the Mie calculated and approximated results at a given RH, respectively.

In the case of AS in the RH range of 37–95%, MAE ranges from 2.03 to 20.16%. For a RH range of 37–90%, MAE ranges from 1.96 to 15.44%.

Along with AS, one of the important factors contributing to regional differences in aerosols in the model is NaCl. The original Malm's reconstructed method included NaCl aerosols in the coarse mode (Malm et al., 1994). Although the total NaCl surface mass concentration is dominated by super-micron particles, solar radiation scattering is more efficient on particle diameters between 0.2 and 1.0 μm as compared to other diameters (Ayash et al., 2008). Sub-micron sea-salt aerosols account for ~20% of the total light scattering (Ayash et al., 2008; Quinn et al., 1996). For this reason, f(RH) for NaCl is important for sub-micron particles as well as for super-micron particles. In this study, we parameterize the f(RH) of NaCl polydispersed aerosols, which include fine and accumulation modes.

Fig. 6(a) shows an f_{Mie}(RH) for NaCl in the range of 47–95% and a different d_g of 0.1, 0.2, 0.7, and 2.5 μm. The f_{Mie}(RH) in Fig. 6(a) is for a GSD of 1.5. f(RH) decreases as d_g increases (Fig. 6). Fig. 6(b) shows f_{Mie}(RH) with different GSDs of 1.5 and 2.5 and a d_g of 0.1, 0.7, and 2.5 μm for NaCl. f_{Mie}(RH) converges as the GSD and d_g increase. Fig. 6(c) and (d) show a comparison between the Mie calculated (f_{Mie}(RH)) and approximated f(RH) (f_{app}(RH)) in the case of NaCl. Comparisons are made between a d_g of 0.1 and 2.5 μm for a GSD of 1.5 and 2.5. Fig. 6(c) and (d) show that the Mie calculated and approximated f(RH) are in good agreement. In the case of NaCl,

Table 2

Approximated coefficients (α, β, γ) for the hygroscopic growth factor of AS $\left(f_{app,AS}(\mathrm{RH}) = \alpha_{AS} + \beta_{AS}\left(\frac{1}{1-RH}\right) + \gamma_{AS}\left(\frac{1}{1-RH}\right)^2\right)$.

Size range	coef. Intercept, α_{AS}	coef. 1/(1-RH), β_{AS}	coef. $1/(1\text{-RH})^2$, γ_{AS}
dgv< 0.3 μm	0.3	0.83	0.07
0.3 μm < dgv<1 μm	(-0.27GSD+0.89)$Log_{10}(d_{gv}/d_{g0})$+0.84	(0.29GSD-0.94)$Log_{10}(d_{gv}/d_{g0})$+0.27	(0.03GSD-0.085)$Log_{10}(d_{gv}/d_{g0})$-0.01
dgv>1 μm	0.85	0.28	0.0

Table 3

Approximated coefficients (α, β, γ) for the hygroscopic growth factor of NaCl $\left(f_{app,\,ss}(\mathrm{RH}) = \alpha_{ss} + \beta_{ss}\left(\frac{1}{1-RH}\right) + \gamma_{ss}\left(\frac{1}{1-RH}\right)^2\right)$.

Size range	coef. Intercept, α_{ss}	coef. 1/(1-RH), β_{ss}	Range	coef. $1/(1\text{-RH})^2$, γ_{ss}
dgv< 0.3 μm	0.00	3.00	dgv<0.01 μm	0.40
0.3 μm < dgv<1 μm	(-0.68GSD+2.29)Log10(dgv/dg0)+1.4	(0.7GSD −2.77)Log10(dgv/dg0)+0.5	0.01 μm < dgv<0.1 μm	(0.31GSD-0.91)($\mathrm{Log_{10}}$(dgv/dg0)+1)
dgv>1 μm	1.35	0.48	dgv>0.1 μm	0.00

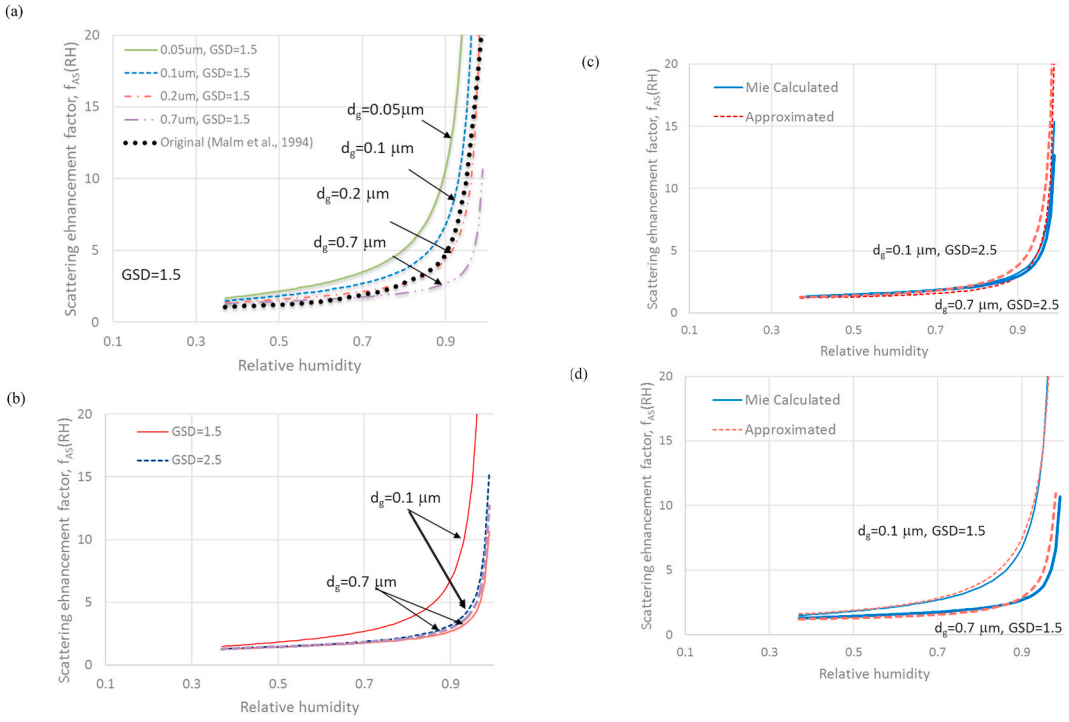

Fig. 5. Aerosol mass concentration and scattering enhancement factor, f(RH), for different size distributions with different GSD and geometric mean diameters (d_g) for AS, with an RH of 37–95%.

MAE ranges from 4.48 to 27.66% for an RH ranging between 47 and 95% and from 3.63 to 27.04% for an RH ranging between 47 and 90%.

Table 4 summarizes MAEs for AS and NaCl. The average MAEs for 27 cases are 7.6% (RH of 37–95%, AS), 5.55% (RH of 37–90%, AS), 9.86% (RH of 37–95%, NaCl), and 8.03% (RH of 37–90%, NaCl).

3.2. Size and type dependency of f(RH)

Many previous studies have shown that different types of aerosols exhibit different hygroscopic, optical and microphysical behaviors, which are affected by aerosol physico-chemical characteristics and other factors, including location, time, aging process, mixing state, and source (Chen et al., 2014; Wang et al., 2018). For example, different types of aerosols, such as biomass-burning and marine aerosols, show different hygroscopic growth factors (Asmi et al., 2010). According to Titos et al. (2016), the highest f(RH) values were measured in clean marine environments, where pollution had a major influence on f(RH). Dust aerosols tend to have the lowest reported hygroscopicity among the aerosol types studied (Titos et al., 2016).

Additional information is required for understanding the size dependency of aerosol hygroscopicity (Chen et al., 2014, 2019; Eichler et al., 2008; Sorooshian et al., 2008; Wang et al., 2018). Different aerosol types tend to have different sizes, depending on their composition and sources. Moreover, although aerosol types are identical, different sizes of particles can undergo different size-dependent processes under ambient conditions, such as coagulation, condensation, and deposition, which results in different hygroscopic growth behaviors. Thus, further experimental and theoretical studies on the particle size-resolved hygroscopic behavior of aerosols are required to understand the mechanisms controlling the evolution of aerosol pollution (Brock et al., 2016; Kuang et al., 2018; Wang et al., 2018).

In this study, the approximated coefficients for both AS and NaCl show that there are sub-micron particle-size ranges that show a

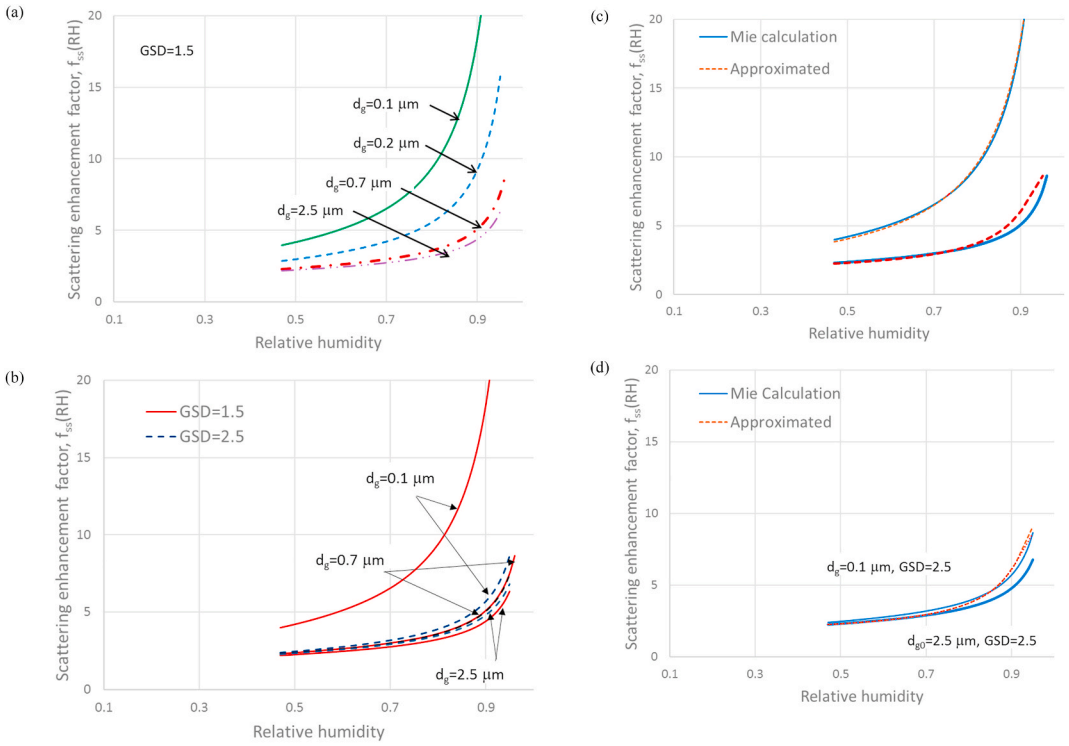

Fig. 6. Aerosol mass concentration and scattering enhancement factor, f(RH), for different size distributions with different GSD and geometric mean diameters (d_g) for NaCl, with an RH of 47–95%.

Table 4
Mean absolute errors (MAE, %) for different size distributions.

			AS		NaCl	
d_g (μm)	d_{gv} (μm)	GSD	MAE (37–95%)	MAE (37–90%)	MAE (47–95%)	MAE (47–90%)
0.01	0.016	1.5	4.76	5.04	7.15	7.12
0.02	0.033		2.04	1.96	14.52	13.83
0.05	0.082		4.29	3.46	27.66	27.04
0.10	0.164		13.07	9.94	11.31	11.15
0.20	0.328		20.17	15.44	10.48	7.50
0.50	0.819		5.10	4.04	10.16	6.85
0.70	1.146		9.97	5.88	15.94	11.26
1.00	1.638		8.49	5.16	9.60	5.96
2.50	4.094		7.45	4.78	7.31	4.38
0.01	0.042	2.0	3.53	3.30	9.26	10.14
0.02	0.085		6.05	4.37	7.81	7.97
0.05	0.211		9.97	7.27	4.49	3.62
0.10	0.423		6.20	4.20	6.93	5.06
0.20	0.845		7.89	7.13	16.10	17.38
0.50	2.113		8.09	4.91	9.09	5.29
0.70	2.959		8.00	4.91	8.53	4.95
1.00	4.226		7.72	4.82	7.77	4.51
2.50	10.566		7.38	4.84	7.27	4.51
0.01	0.124	2.5	5.46	5.49	5.69	5.77
0.02	0.248		5.34	5.31	5.83	6.10
0.05	0.621		10.05	9.00	16.24	17.21
0.10	1.241		6.17	4.52	7.20	6.04
0.20	2.483		7.23	4.58	7.36	4.35
0.50	6.207		7.67	4.80	7.79	4.53
0.70	8.689		7.59	4.81	7.60	4.47
1.00	12.413		7.53	4.83	7.56	4.51
2.50	31.033		8.07	4.98	9.37	5.32

size dependency of these coefficients. For a sub-micron size range, for example, an increase in particle size would lead to a lower f(RH) for both AS and NaCl. Here, it should be noted that f(RH) is based on the assumption that aerosols are externally mixed.

For the overall f(RH) of internally mixed aerosols, however, there has been an ongoing discussion regarding the size dependency. If we consider internally mixed aerosols to be composed of hygroscopic and non-hygroscopic species, the overall f(RH) depends on the fraction of hygroscopic aerosol species. Generally, the fractions of aerosol species determine aerosol types and, thus, the f(RH) of internally mixed aerosols is type dependent. For example, f(RH) values are larger for marine sites compared to other environments due to the high hygroscopicity of NaCl (Titos et al., 2016; Zieger et al., 2011).

Aerosol mixtures are related to aerosol type and f(RH) depends on the fractions of hygroscopic species with different hygroscopic properties. If we calculate f(RH) for an internal mixing, also the volume fraction of the chemical composition will have an influence. For example, an increase in the organic fraction, which is known to be weakly hygroscopic (Malm et al., 2005; Wang et al., 2018), will lower the f(RH) of internally mixed aerosols.

Thus, the size dependency of f(RH) is related to the fraction of each aerosol and the degree of aerosol hygroscopicity (Zieger et al., 2013). Zieger et al. (2010) indicated that small and less hygroscopic aerosols can have the same f(RH) as large and more hygroscopic aerosols due to the compensation between size and hygroscopicity. According to Zieger et al. (2010), for example, the observed f(RH) did not show a clear seasonal trend and was not positively correlated with the occurrence of sea salt, as inferred from the volume fraction of large particles. This compensation can be seen in the Mie calculations for aerosols consisting of various fractions of highly and weakly hygroscopic inorganic aerosols (Zieger et al., 2010). Other studies (Sheridan et al., 2001; Titos et al., 2016) showed that a behavior as a function of size is more evident in clean than in polluted marine situations and that the difference between f(RH) for different size cuts was more obvious for clean marine conditions. From these previous studies, it can be inferred that the size dependency of f(RH) depends on many environment-related physico-chemical parameters, which make the quantification of f(RH) difficult. Clearly, more studies on this size dependency, using observations and experimental frameworks, are required.

4. Conclusions

In this study, we developed analytical expressions to approximate f(RH) for ammonium sulfate and sea salt aerosols. To obtain these values, we first computed mass growth factors based on aerosol thermodynamic models. Then, the optical properties of the aerosols were calculated using the Mie theory for a range of different aerosol properties and size distributions. From these obtained values, f(RH) was approximated for polydispersed aerosols as a quadratic function of RH and the coefficients were parameterized as a function of d_{gv} and GSD.

The results show that the obtained approximated coefficients and f(RH) correspond well with the Mie calculated values for the polydispersed particle sizes. Consequently, this study suggests a simple and accurate formula for f(RH). This formula estimates f(RH) and related optical properties, such as the aerosol extinction coefficient and AOD, with confidence.

The current approximated coefficients for f(RH) (f_{app}(RH)) are based on a quadratic curve following Malm et al. (1994). There are many different formulas for the parameterization of f(RH); however, it should be noted that the previously proposed empirical expressions for f(RH) depend only on RH.

To the best of our knowledge, this study is the first to parametrize the size dependency of f(RH) for polydisperse aerosols. However, there remains a need for further investigation into more accurate, simple, and optimized methods, which will contribute towards improving hygroscopic studies. To consider size-resolved aerosol optical properties, such as extinction and scattering coefficients, mass scattering efficiency should be expressed as a function of size. We will perform a more intensive investigation into the parameterization of the size-dependent mass scattering efficiency in a follow-up study. It should also be noted that our parameterization covers the entire size range, including Aitken and accumulation modes, but neglects Kelvin effects, which needs to be improved when considering curvature effects.

There has been an ongoing discussion about the size dependency of f(RH) in the real atmosphere. f(RH) under real conditions depends on many factors, such as mixture- and hygroscopicity-related environmental and meteorological parameters. This study focused on aerosol sizes among those factors and, hence, to isolate the size dependency of f(RH), other factors have to be theoretically and experimentally confined.

Declaration of competing interest

The authors declare that they have no known competing financial interests or personal relationships that could have appeared to influence the work reported in this paper.

Acknowledgments

This research was supported by the Technology Development Program to Solve Climate Changes through the National Research Foundation of Korea (NRF) funded by the Ministry of Science, ICT (2019M1A2A2103953). This study was also supported by the KOPRI program (PN20081), funded by a National Research Foundation of Korea Grant (NRF-2016M1A5A1901786) and by the National Strategic Project – Fine particle of the National Research Foundation of Korea (NRF) funded by the Ministry of Science and ICT (MSIT), the Ministry of Environment (ME), and the Ministry of Health and Welfare (MOHW) (NRF-2017M3D8A1092022). It was supported by the National Research Foundation of Korea (NRF) grant funded by the Korea government (MSIT) (No. 2020R1A2C101327811).

References

Asmi, E., Frey, A., Virkkula, A., Ehn, M., Manninen, H. E., Timonen, H., Tolonen-Kivimäki, O., Aurela, M., Hillamo, R., & Kulmala, M. (2010). Hygroscopicity and chemical composition of Antarctic sub-micrometre aerosol particles and observations of new particle formation. *Atmospheric Chemistry and Physics, 10*, 4253–4271. https://doi.org/10.5194/acp-10-4253-2010.

Ayash, T., Gong, S., & Jia, C. Q. (2008). Direct and indirect shortwave radiative effects of sea salt aerosols. *Journal of Climate, 21*, 3207–3220. https://doi.org/10.1175/2007JCLI2063.1.

Brock, C. A., Wagner, N. L., Anderson, B. E., Beyersdorf, A., Campuzano-Jost, P., Day, D. A., Diskin, G. S., Gordon, T. D., Jimenez, J. L., Lack, D. A., Liao, J., Markovic, M. Z., Middlebrook, A. M., Perring, A. E., Richardson, M. S., Schwarz, J. P., Welti, A., Ziemba, L. D., & Murphy, D. M. (2016). Aerosol optical properties in the southeastern United States in summer – Part 2: Sensitivity of aerosol optical depth to relative humidity and aerosol parameters. *Atmospheric Chemistry and Physics, 16*, 5009–5019. https://doi.org/10.5194/acp-16-5009-2016.

Carrico, C. M., Kus, P., Rood, M. J., Quinn, P. K., & Bates, T. S. (2003). Mixtures of pollution, dust, sea salt, and volcanic aerosol during ACE-Asia: Radiative properties as a function of relative humidity. *Journal of Geophysical Research, 108*(D23), 8650. https://doi.org/10.1029/2003JD003405.

Cheng, Y. F., Wiedensohler, A., Eichler, H., Heintzenberg, J., Tesche, M., Ansmann, A., Wendisch, M., Su, H., Althausen, D., Herrmann, H., Gnauk, T., Brüggemann, E., Hu, M., & Zhang, Y. H. (2008). Relative humidity dependence of aerosol optical properties and direct radiative forcing in the surface boundary layer at Xinken in Pearl River Delta of China: An observation based numerical study. *Atmospheric Environment, 42*, 6373–6397. https://doi.org/10.1016/j.atmosenv.2008.04.009.

Chen, J., Li, Z., Lv, M., Wang, Y., Wang, W., Zhang, Y., Wang, H., Yan, X., Sun, Y., & Cribb, M. (2019). Aerosol hygroscopic growth, contributing factors, and impact on haze events in a severely polluted region in northern China. *Atmospheric Chemistry and Physics, 19*, 1327–1342. https://doi.org/10.5194/acp-19-1327-2019.

Chen, J., Zhao, C. S., Ma, N., & Yan, P. (2014). Aerosol hygroscopicity parameter derived from the light scattering enhancement factor measurements in the North China Plain. *Atmospheric Chemistry and Physics, 14*, 8105–8118. https://doi.org/10.5194/acp-14-8105-2014.

Clegg, S., Seinfeld, J., & Edney, E. (2003). Thermodynamic modelling of aqueous aerosols containing electrolytes and dissolved organic compounds. II. An extended Zdanovskii–Stokes–Robinson approach. *Journal of Aerosol Science, 34*, 667–690. https://doi.org/10.1016/s0021-8502(03)00019-3.

Covert, D. S., Charlson, R. J., & Ahlquist, N. C. (1972). A study of the relationship of chemical composition and humidity to light scattering by aerosols. *Journal of Applied Meteorology, 11*, 968–976. https://doi.org/10.1175/1520-0450(1972)011%3C0968:ASOTRO%3E2.0.CO.

Day, D. E., Malm, W. C., & Kreidenweis, S. M. (2000). Aerosol light scattering measurements as a function of relative humidity. *Journal of the Air & Waste Management Association, 50*, 710–716. https://doi.org/10.1080/10473289.2000.10464103.

Deng, H., Tan, H., Li, F., Cai, M., Chan, P. W., Xu, H., Huang, X., & Wu, D. (2016). Impact of relative humidity on visibility degradation during a haze event: A case study. *The Science of the Total Environment, 569*, 1149–1158. https://doi.org/10.1016/j.scitotenv.2016.06.190.

Eichler, H., Cheng, Y. F., Birmili, W., Nowak, A., Wiedensohler, A., Brüggemann, E., Gnauk, T., Herrmann, H., Althausen, D., Ansmann, A., Engelmann, R., Tesche, M., Wendisch, M., Zhang, Y. H., Hu, M., Liu, S., & Zeng, L. M. (2008). Hygroscopic properties and extinction of aerosol particles at ambient relative humidity in South-Eastern China. *Atmospheric Environment, 42*(25), 6321–6334. https://doi.org/10.1016/j.atmosenv.2008.05.007.

Ghan, S. J., Liu, X., Easter, R. C., Zaveri, R., Rasch, P. J., Yoon, J.-H., & Eaton, B. E. (2012). Toward a minimal representation of aerosols in climate models: Comparative decomposition of aerosol direct, semidirect, and indirect radiative forcing. *Journal of Climate, 25*, 6461–6476. https://doi.org/10.1175/JCLI-D-11-00650.1.

Ghan, S. J., & Zaveri, R. A. (2007). Parameterization of optical properties for hydrated internally mixed aerosol. *Journal of Geophysical Research, 112*, D10201. https://doi.org/10.1029/2006JD007927.

Habyarimana, E., Piccard, I., Catellani, M., De Franceschi, P., & Dall'Agata, M. (2019). Towards predictive modeling of sorghum biomass yields using fraction of absorbed photosynthetically active radiation derived from sentinel-2 satellite imagery and supervised machine learning techniques. *Agronomy, 9*, 203.

Hand, J. L., & Malm, W. C. (2007). Review of aerosol mass scattering efficiencies from ground-based measurements since 1990. *Journal of Geophysical Research, 112*, D16203. https://doi.org/10.1029/2007jd008484.

Hand, J. L., Prenni, A. J., Schichtel, B. A., Malm, W. C., & Chow, J. C. (2019). Trends in remote PM2.5 residual mass across the United States: Implications for aerosol mass reconstruction in the IMPROVE network. *Atmospheric Environment, 203*, 141–152. https://doi.org/10.1016/j.atmosenv.2019.01.049.

Hänel, G. (1981). An attempt to interpret the humidity dependencies of the aerosol extinction and scattering coefficients. *Atmospheric Environment, 15*(3), 403–406. https://doi.org/10.1016/0004-6981(81)90045-7.

Hinds, W. C. (1999). *Aerosol Technology: Properties, behavior, and measurement of airborne particles* (2nd ed.). New York: John Wiley & Sons.

van de Hulst, H. C. (1981). *Light scattering by small particles*. New York: Dover.

Im, J. S., Saxena, V. K., & Wenny, B. N. (2001). An assessment of hygroscopic growth factors for aerosols in the surface boundary layer for computing direct radiative forcing. *Journal of Geophysical Research, 106*(D17), 20213–20224. https://doi.org/10.1029/2000jd000152.

Jung, C. H., Lee, J. Y., Um, J., Lee, S. S., Yoon, Y. J., & Kim, Y. P. (2019). Estimation of source-based aerosol optical properties for polydisperse aerosols from receptor models. *Applied Sciences, 9*, 1443.

Jung, C. H., Um, J., Bae, S. Y., Yoon, Y. J., Lee, S. S., Lee, J. Y., & Kim, Y. P. (2018). Analytic expression for the aerosol mass efficiencies for polydispersed accumulation mode. *Aerosol Air Qual. Res., 18*, 1503–1514. https://doi.org/10.4209/aaqr.2018.02.0067.

Kasten, F. (1969). Visibility forecast in the phase of pre-condensation. *Tellus, 21*(5), 631–635.

Kiehl, J. T., Schneider, T. L., Rasch, P. J., Barth, M. C., & Wong, J. (2000). Radiative forcing due to sulfate aerosols from simulations with the National Center for atmospheric research community climate model version 3. *Journal of Geophysical Research, 105*(D1), 1441–1457. https://doi.org/10.1029/1999JD900495.

Kotchenruther, R. A., & Hobbs, P. V. (1998). Humidification factors of aerosols from biomass burning in Brazil. *Journal of Geophysical Research, 103*, D24. https://doi.org/10.1029/98JD00340, 32081–32089.

Kreidenweis, S. M., Koehler, K., DeMott, P. J., Prenni, A. J., Carrico, C., & Ervens, B. (2005). Water activity and activation diameters from hygroscopicity data —part I: Theory and application to inorganic salts. *Atmospheric Chemistry and Physics, 5*, 1357–1370. https://doi.org/10.5194/acp-5-1357-2005.

Kreidenweis, S. M., Petters, M., & DeMott, P. (2008). Single-parameter estimates of aerosol water content. *Environmental Research Letters, 3*, Article 035002. https://doi.org/10.1088/1748-9326/3/3/035002.

Kuang, Y., Zhao, C. S., Tao, J. C., Bian, Y. X., & Ma, N. (2016). Impact of aerosol hygroscopic growth on the direct aerosol radiative effect in summer on North China Plain. *Atmospheric Environment, 147*, 224–233. https://doi.org/10.1016/j.atmosenv. 2016.10.013.

Kuang, Y., Zhao, C. S., Zhao, G., Tao, J. C., Xu, W., Ma, N., & Bian, Y. X. (2018). A novel method for calculating ambient aerosol liquid water content based on measurements of a humidified nephelometer system. *Atmos. Meas. Tech., 11*, 2967–2982. https://doi.org/10.5194/amt-11-2967-2018.

Lagrosas, N., Bagtasa, G., Manago, N., & Kuze, H. (2019). Influence of ambient relative humidity on seasonal trends of the scattering enhancement factor for aerosols in chiba, Japan. *Aerosol Air Qual. Res., 19*, 1856–1871. https://doi.org/10.4209/aaqr.2018.07.0267.

Laskina, O., Morris, H. S., Grandquist, J. R., Qin, Z., Stone, E. A., Tivanski, A. V., & Grassian, V. H. (2015). Size matters in the water uptake and hygroscopic growth of atmospherically relevant multicomponent aerosol particles. *The Journal of Physical Chemistry A, 119*(19), 4489–4497. https://doi.org/10.1021/jp510268p.

Leibensperger, E. M., Mickley, L. J., Jacob, D. J., Chen, W.-T., Seinfeld, J. H., Nenes, A., Adams, P. J., Streets, D. G., Kumar, N., & Rind, D. (2012). Climatic effects of 1950–2050 changes in US anthropogenic aerosols – Part 1: Aerosol trends and radiative forcing. *Atmospheric Chemistry and Physics, 12*, 3333–3348. https://doi.org/10.5194/acp-12-3333-2012.

Liu, J., Bergin, M., Guo, H., King, L., Kotra, N., Edgerton, E., & Weber, R. J. (2013). Size-resolved measurements of brown carbon in water and methanol extracts and estimates of their contribution to ambient fine-particle light absorption. *Atmospheric Chemistry and Physics, 13*, 12389–12404. https://doi.org/10.5194/acp-13-12389-2013.

Liu, X. G., Cheng, Y. F., Zhang, Y. H., Jung, J., Sugimoto, N., Chang, S.-Y., Kim, Y. J., Fan, S., & Zeng, L. (2008). Influences of relative humidity and particle chemical composition on aerosol scattering properties during the 2006 PRD campaign. *Atmospheric Environment, 42*, 1525–1536. https://doi.org/10.1016/j.atmosenv.2007.10.077.

Liu, Q., Liu, D., Gao, Q., Tian, P., Wang, F., Zhao, D., Bi, K., Wu, Y., Ding, S., Hu, K., Zhang, J., Ding, D., & Zhao, C. (2020). Vertical characteristics of aerosol hygroscopicity and impacts on optical properties over the North China Plain during winter. *Atmospheric Chemistry and Physics, 20*, 3931–3944. https://doi.org/10.5194/acp-20-3931-2020.

Liu, X. G., Zhang, Y. H., Jung, J., Gu, J., Li, Y., Guo, S., Chang, S.-Y., Yue, D., Lin, P., Kim, Y. J., Hu, M., Zeng, L., & Zhu, T. (2009). Research on the hygroscopic properties of aerosols by measurement and modeling during CAREBeijing-2006. *Journal of Geophysical Research, 114*, D00G16. https://doi.org/10.1029/2008JD010805.

Malm, W. C. (2016). *Visibility: The seeing of near and distant landscape features*. Elsevier.

Malm, W. C., & Day, D. E. (2001). Estimates of aerosol species scattering characteristics as 975 a function of relative humidity. *Atmospheric Environment, 35*, 2845–2860.

Malm, W. C., Day, D. E., Kreidenweis, S. M., Collet, J. L., & Lee, T. (2003). Humidity-977 dependent optical properties of fine particles during the big bend regional aerosol 978 and visibility observational study. *Journal of Geophysical Research, 108*(D9), 4279.

Malm, W. C., Day, D. E., Kreidenweis, S. M., Collett, J. L., Jr., Carrico, C., McMeeking, G., & Lee, T. (2005). Hygroscopic properties of an organic-laden aerosol. *Atmospheric Environment, 39*, 4969–4982.

Malm, W. C., Sisler, J. F., Huffman, D., Eldred, R. A., & Cahill, T. A. (1994). Spatial and seasonal trends in particle concentration and optical extinction in the United States. *Journal of Geophysical Research, 99*(D1), 1347–1370.

Matta, C. F., Massa, L., Gubskaya, A. V., & Knoll, E. (2011). Can one take the logarithm or the sine of a dimensioned quantity or a unit? Dimensional analysis involving transcendental functions. *Journal of Chemical Education, 88*(1), 67–70. https://pubs.acs.org/doi/pdf/10.1021/ed1000476.

Molnár, Á., Imre, K., Ferenczi, Z., Kiss, G., & Gelencser, A. (2020). Aerosol hygroscopicity: Hygroscopic growth proxy based on visibility for low-cost PM monitoring. *Atmospheric Research, 236*, Article 104815.

Musante, C., Schroeter, J., Rosati, J., Crowder, T., Hickey, A., & Martonen, T. (2002). Factors affecting the deposition of inhaled porous drug particles. *Journal of Pharmaceutical Sciences*, (7), 1590–1600. https://doi.org/10.1002/jps.10152.

Ogawa, S., Setoguchi, Y., Kawana, K., Nakayama, T., Ikeda, Y., Sawada, Y., Matsumi, Y., & Mochida, M. (2016). Hygroscopicity of aerosol particles and CCN activity of nearly hydrophobic particles in the urban atmosphere over Japan during summer. *Journal of Geophysical Research - D: Atmospheres, 121*, 7215–7234. https://doi.org/10.1002/2015JD024636.

Pan, X. L., Yan, P., Tang, J., Ma, J. Z., Wang, Z. F., Gbaguidi, A., & Sun, Y. L. (2009). Observational study of influence of aerosol hygroscopic growth on scattering coefficient over rural area near Beijing mega-city. *Atmospheric Chemistry and Physics, 9*, 7519–7530. https://doi.org/10.5194/acp-9-7519-2009.

Petters, M. D., & Kreidenweis, S. M. (2007). A single parameter representation of hygroscopic growth and cloud condensation nucleus activity. *Atmospheric Chemistry and Physics, 7*, 1961–1971. https://doi.org/10.5194/acp-7-1961-2007.

Pitchford, M., Malm, W., Schichtel, B., Kumar, N., Lowenthal, D., & Hand, J. (2007). Revised algorithm for estimating light extinction from IMPROVE particle speciation data. *Journal of the Air & Waste Management Association, 57*(11), 1326–1336. https://doi.org/10.3155/1047-3289.57.11.1326.

Qi, X. F., Sun, J. Y., Zhang, L., Shen, X. J., Zhang, X. Y., Zhang, Y. M., Wang, Y. Q., Che, H. C., Zhang, Z. X., Zhong, J. T., Tan, K. Y., Zhao, H. R., & Ren, S. X. (2018). Aerosol hygroscopicity during the haze red-alert period in December 2016 at a rural site of the north China plain. *J. Meteo. Res., 32*, 38–48.

Quinn, P. K., Anderson, T. L., Bates, T., Dlugi, R., Heintzenberg, J., Hoyningen-Huene, W., Kulmala, M., Russell, P., & Swietlicki, E. (1996). Closure in tropospheric aerosol-climate research: A review and future needs for addressing aerosol direct shortwave radiative forcing. *Contributions to Atmospheric Physics, 69*, 547–577.

Randriamiarisoa, H., Chazette, P., Couvert, P., Sanak, J., & Mégie, G. (2006). Relative humidity impact on aerosol parameters in a Paris suburban area. *Atmospheric Chemistry and Physics, 6*, 1389–1407. https://doi.org/10.5194/acp-6-1389-2006.

Rissler, J., Vestin, A., Swietlicki, E., Fisch, G., Zhou, J., Artaxo, P., & Andreae, M. O. (2006). Size distribution and hygroscopic properties of aerosol particles from dry-season biomass burning in Amazonia. *Atmospheric Chemistry and Physics, 6*, 471–491. https://doi.org/10.5194/acp-6-471-2006.

Seinfeld, J. H., & Pandis, S. N. (1998). *Atmospheric chemistry and physics: From air pollution to climate change*. John Wiley.

Shen, X. J., Sun, J. Y., Zhang, X. Y., Zhang, Y. M., Wang, Y. Q., Tan, K. Y., Wang, P., Zhang, L., Qi, X. F., Che, H. C., Zhang, Z. X., Zhong, J. T., Zhao, H. R., & Ren, S. X. (2018). Comparison of submicron particles at a rural and an urban site in the North China Plain during the December 2016 heavy pollution episodes. *J. Meteo. Res., 32*, 26–37.

Sheridan, P. J., Delene, D. J., & Ogren, J. A. (2001). Four years of continuous surface aerosol measurements from the department of energy's atmospheric radiation measurement program southern great plains cloud and radiation testbed site. *Journal of Geophysical Research, 106*, D18. https://doi.org/10.1029/2001JD000785, 20735–20747.

Sorooshian, A., Hersey, S., Brechtel, F. J., Corless, A., Flagan, R. C., & Seinfeld, J. H. (2008). Rapid, size-resolved aerosol hygroscopic growth measurements: Differential aerosol sizing and hygroscopicity spectrometer probe (DASH-SP). *Aerosol Science and Technology, 42*(6), 445–464. https://doi.org/10.1080/02786820802178506.

IPCC. (2013). Cambridge, United Kingdom and New York. In T. F. Stocker, D. Qin, G.-K. Plattner, M. Tignor, S. K. Allen, J. Boschung, A. Nauels, Y. Xia, V. Bex, & P. M. Midgley (Eds.), *Climate change 2013: The physical science basis. Contribution of working group I to the fifth assessment report of the intergovernmental panel on climate change*.

Swietlicki, E., Hansson, H.-C., Hämeri, K., Svenningsson, B., Massling, A., McFiggans, G., McMurry, P. H., Petäjä, T., Tunved, P., Gysel, M., Topping, D., Weingartner, E., Baltensperger, U., Rissler, J., Wiedensohler, A., & Kulmala, M. (2008). Hygroscopic properties of submicrometer atmospheric aerosol particles measured with H-TDMA instruments in various environments-a review. *Tellus B: Chemical and Physical Meteorology, 60*(3), 432–469.

Tao, J., Zhang, L., Cao, J., & Zhang, R. (2017). A review of current knowledge concerning PM2. 5 chemical composition, aerosol optical properties and their relationships across China. *Atmospheric Chemistry and Physics, 17*, 9485–9518. https://doi.org/10.5194/acp-17-9485-2017.

Titos, G., Cazorla, A., Zieger, P., Andrews, E., Lyamani, H., Granados-Muñoz, M. J., Olmo, F. J., & Alados-Arboledas, L. (2016). Effect of hygroscopic growth on the aerosol light-scattering coefficient: A review of measurements, techniques and error sources. *Atmospheric Environment, 141*, 494–507. https://doi.org/10.1016/j.atmosenv.2016.07.021.

Twohy, C. H., Coakley, J. A., Jr., & Tahnk, W. R. (2009). Effect of changes in relative humidity on aerosol scattering near clouds. *Journal of Geophysical Research, 114*, D05205. https://doi.org/10.1029/2008JD010991.

Wang, X., Shen, X. J., Sun, J. Y., Zhang, X. Y., Wang, Y. Q., Zhang, Y. M., Wang, P., Xia, C., Qi, X. F., & Zhong, J. T. (2018). Size-resolved hygroscopic behavior of atmospheric aerosols during heavy aerosol pollution episodes in Beijing in December 2016. *Atmospheric Environment, 194*, 188–197. https://doi.org/10.1016/j.atmosenv.2018.09.041.

Xu, J., Bergin, M. H., Yu, X., Liu, G., Zhao, J., Carrico, C. M., & Baumann, K. (2002). Measurement of aerosol chemical, physical and radiative properties in the Yangtze delta region of China. *Atmospheric Environment, 36*(2), 161–173. https://doi.org/10.1016/S1352-2310(01)00455-1.

Yan, P., Pan, X. L., Tang, J., Zhou, X. J., Zhang, R. J., & Zeng, L. M. (2009). Hygroscopic growth of aerosol scattering coefficient: A comparative analysis between urban and suburban sites at winter in beijing. *Particuology, 7*, 52–60. https://doi.org/10.1016/j.partic.2008.11.009.

Zhang, Y. H., Hu, M., Zhong, L. J., Wiedensohler, A., Liu, S. C., Andreae, M. O., Wang, W., & Fan, S. J. (2008). Regional integrated experiments on air quality over pearl river delta 2004 (PRIDE-PRD2004): Overview. *Atmospheric Environment, 42*, 6157–6173. https://doi.org/10.1016/j.atmosenv.2008.03.025.

Zhang, X., Massoli, P., Quinn, P. K., Bates, T. S., & Cappa, C. D. (2014). Hygroscopic growth of submicron and supermicron aerosols in the marine boundary layer. *Journal of Geophysical Research in the Atmosphere, 119*, 8384–8399. https://doi.org/10.1002/2013JD021213.

Zhang, L., Sun, J. Y., Shen, X. J., Zhang, Y. M., Che, H. C., Ma, Q. L., Zhang, Y. W., Zhang, X. Y., & Ogren, J. A. (2015). Observations of relative humidity effects on aerosol light scattering in the Yangtze River Delta of China. *Atmospheric Chemistry and Physics, 1075*, 8439–8454. https://doi.org/10.5194/acpd-15-2853-2015.

Zhang, Y., Wang, Y., Zhang, X., et al. (2018). Chemical components, variation, and source identification of PM1 during the heavy air pollution episodes in beijing in december 2016. *J Meteorol Res, 32*, 1–13. https://doi.org/10.1007/s13351-018-7051-8.

Zieger, P., Fierz-Schmidhauser, R., Gysel, M., Ström, J., Henne, S., Yttri, K. E., Baltensperger, U., & Weingartner, E. (2010). Effects of relative humidity on aerosol light scattering in the Arctic. *Atmospheric Chemistry and Physics, 10*, 3875–3890. https://doi.org/10.5194/acp-10-3875-2010.

Zieger, P., Fierz-Schmidhauser, R., Weingartner, E., & Baltensperger, U. (2013). Effects of relative humidity on aerosol light scattering: Results from different European sites. *Atmospheric Chemistry and Physics, 13*, 10609–10631. https://doi.org/10.5194/acp-13-10609-2013.

Zieger, P., Schmidhauser, R. F., Poulain, L., Müller, T., Birmili, W., Spindler, G., Wiedensohler, A., Baltensperger, U., & Weingartner, E. (2014). Influence of water uptake on the aerosol particle light scattering coefficients of the Central European aerosol. *Tellus B: Chemical and Physical Meteorology, 66*(1). https://doi.org/10.3402/tellusb.v66.22716.

Zieger, P., Weingartner, E., Henzing, J., Moerman, M., de Leeuw, G., Mikkilä, J., Ehn, M., Petäjä, T., Clémer, K., van Roozendael, M., Yilmaz, S., Frieβ, U., Irie, H., Wagner, T., Shaiganfar, R., Beirle, W., Apituley, A., Wilson, K., & Baltensperger, U. (2011). Comparison of ambient aerosol extinction coefficients obtained from in-situ, MAX-DOAS and LIDAR measurements at Cabauw. *Atmospheric Chemistry and Physics, 11*, 2603–2624. https://doi.org/10.5194/acp-11-2603-2011.